

# Chemokine Cxcl9 Attenuates Liver Fibrosis-Associated Angiogenesis in Mice

Hacer Sahin,<sup>1</sup> Erawan Borkham-Kamphorst,<sup>2</sup> Christoph Kuppe,<sup>3</sup> Mirko Moreno Zaldivar,<sup>1</sup> Christoph Grouls,<sup>4</sup> Muhammad Al-samman,<sup>1</sup> Andreas Nellen,<sup>1</sup> Petra Schmitz,<sup>1</sup> Daniel Heinrichs,<sup>1</sup> Marie-Luise Berres,<sup>1</sup> Dennis Doleschel,<sup>4</sup> David Scholten,<sup>1</sup> Ralf Weiskirchen,<sup>2</sup> Marcus J. Moeller,<sup>3</sup> Fabian Kiessling,<sup>4</sup> Christian Trautwein,<sup>1</sup> and Hermann E. Wasmuth<sup>1</sup>

Recent data suggest that the chemokine receptor CXCR3 is functionally involved in fibroproliferative disorders, including liver fibrosis. Neoangiogenesis is an important pathophysiological feature of liver scarring, but a functional role of angiostatic CXCR3 chemokines in this process is unclear. We therefore investigated neoangiogenesis in carbon tetrachloride (CCl<sub>4</sub>)-induced liver fibrosis in *Cxcr3*<sup>-/-</sup> and wildtype mice by histological, molecular, and functional imaging methods. Furthermore, we assessed the direct role of vascular endothelial growth factor (VEGF) overexpression on liver angiogenesis and the fibroproliferative response using a Tet-inducible bitransgenic mouse model. The feasibility of attenuation of angiogenesis and associated liver fibrosis by therapeutic treatment with the angiostatic chemokine Cxcl9 was systematically analyzed *in vitro* and *in vivo*. The results demonstrate that fibrosis progression in *Cxcr3*<sup>-/-</sup> mice was strongly linked to enhanced neoangiogenesis and VEGF/VEGFR2 expression compared with wildtype littermates. Systemic VEGF overexpression led to a fibrogenic response within the liver and was associated with a significantly increased Cxcl9 expression. *In vitro*, Cxcl9 displayed strong antiproliferative and antimigratory effects on VEGF-stimulated endothelial cells and stellate cells by way of reduced VEGFR2 (KDR), phospholipase C<sub>γ</sub> (PLC<sub>γ</sub>), and extracellular signal-regulated kinase (ERK) phosphorylation, identifying this chemokine as a direct counter-regulatory molecule of VEGF signaling within the liver. Accordingly, systemic administration of Cxcl9 led to a strong attenuation of neoangiogenesis and experimental liver fibrosis *in vivo*. **Conclusion:** The results identify direct angiostatic and antifibrotic effects of the *Cxcr3* ligand Cxcl9 in a model of experimental liver fibrosis. The amelioration of liver damage by systemic application of Cxcl9 might offer a novel therapeutic approach for chronic liver diseases associated with increased neoangiogenesis. (HEPATOLOGY 2012;55:1610-1619)

The pathophysiology of liver fibrosis is a complex biological process which includes features of abnormal inflammatory wound healing, the deposition of extracellular matrix proteins, and increased neoangiogenesis.<sup>1-3</sup> At advanced stages, liver fibrosis leads to liver failure, portal hypertension, and represents the main risk factor for hepatocellular carcinoma.<sup>4</sup> Therefore, novel therapies that target key mol-

ecules involved in fibrosis progression are clinically warranted.

A chemokine receptor that has been implicated in many pathophysiological processes of fibroproliferative disorders, including liver fibrosis, is CXCR3.<sup>5,6</sup> The main ligands of this receptor are the interferon- $\gamma$ -inducible chemokines CXCL9, CXCL10, and CXCL11 and the platelet-derived chemokine CXCL4 in

Abbreviations:  $\alpha$ -SMA, alpha smooth muscle actin; AUC, area under the curve; CCl<sub>4</sub>, carbon tetrachloride; ERK, extracellular signal-regulated kinase; IFN- $\gamma$ , interferon-gamma; JNK, c-Jun N-terminal kinase; PLC<sub>γ</sub>, phospholipase C<sub>γ</sub>; ROI, region of interest; rtTA, reverse tetracycline dependent transactivator; VEGF, vascular endothelial growth factor; VEGFR, VEGF receptor; vWF, von Willebrand factor; WT, wildtype.

From the <sup>1</sup>Medical Department III; <sup>2</sup>Institute of Clinical Chemistry and Pathobiochemistry; <sup>3</sup>Medical Department II; <sup>4</sup>Department of Experimental Molecular Imaging, University Hospital Aachen, Aachen, Germany.

Received April 27, 2011; accepted November 25, 2011.

Supported by grants from the Deutsche Forschungsgemeinschaft (WA 2557/2-1 and SFB/TRR 57 P08 to H.E.W. and P17 to M.J.M.) and the Else Kröner-Fresenius Stiftung (to H.E.W.).

Address reprint requests to: Hermann E. Wasmuth, M.D., Medical Department III, University Hospital Aachen, RWTH Aachen, Pauwelsstrasse 30, D-52057 Aachen, Germany. E-mail: hwasmuth@ukaachen.de; fax: ++49 241 8082455.

humans. In experimental murine liver fibrosis models, genetic deletion of *Cxcr3* (*Cxcr3*<sup>-/-</sup>) leads to a reduced hepatic infiltration of interferon- $\gamma$ -positive T-cells,<sup>7</sup> which are considered part of an antifibrotic immune response.<sup>8</sup> These results are congruent with the main role of CXCL9 for transendothelial migration of T helper 1 (T<sub>h</sub>1)-polarized cells into the liver.<sup>9</sup> Furthermore, *Cxcr3* has been shown to be important for recruitment of CD4<sup>+</sup>CD25<sup>+</sup> T regulatory cells into the liver, which might limit inflammatory hepatic injury.<sup>10,11</sup> *In vivo*, the absence of *Cxcr3* leads to pronounced liver fibrosis<sup>7</sup> and an exacerbated liver damage after Concanavalin A administration.<sup>11</sup> These findings are in line with previous studies showing an enhanced fibrogenic response of *Cxcr3*-deficient mice in the lung<sup>12</sup> and the kidney.<sup>13</sup>

Neoangiogenesis and the development of an abnormal angioarchitecture in the liver are strongly linked with progressive fibrogenesis, although the direct interaction between both processes is not yet fully understood.<sup>14</sup> Among molecules involved in angiogenesis, vascular endothelial growth factor (VEGF) has been identified to play potent angiogenic as well as profibrogenic role during liver fibrogenesis.<sup>2,15</sup> In line with these findings, receptors for VEGF (VEGFR) are expressed in liver sinusoidal endothelial and stellate cells.<sup>14</sup> Interestingly, the CXC family of chemokines is also known to be crucially involved in angiogenesis. Members of the CXC family that contain an ELR motif (ELR<sup>+</sup> chemokines) promote angiogenesis, whereas ELR<sup>-</sup> chemokines, which are all ligands of CXCR3, antagonize the formation of new blood vessels.<sup>5,16</sup> Notably, the angiostatic CXCR3 ligand CXCL4 directly interferes with VEGF signaling in human cells.<sup>17</sup> In light of the strong interplay between angiogenesis and fibrosis, these angiostatic features support that this family of chemokines might include important regulators of chronic liver diseases. This hypothesis is supported by earlier studies demonstrating an amelioration of experimental pulmonary angiogenesis by systemic administration of Cxcl10 and Cxcl11 in mice,<sup>16,18</sup> but no studies in experimental liver diseases have yet been performed.

Based on this scientific background, we aimed at characterizing neoangiogenesis in *Cxcr3*<sup>-/-</sup> and wild-type (WT) mice after carbon tetrachloride (CCl<sub>4</sub>)-induced liver fibrosis and to investigate the feasibility of modifying neoangiogenesis and fibrogenesis by sys-

temic administration of the angiostatic *Cxcr3* ligand *Cxcl9* *in vivo*.

## Materials and Methods

**In Vivo Experiments.** C57BL/6 WT, *Cxcr3*<sup>-/-</sup>, and their littermates (backcrossed for more than 10 generations onto the C57BL/6 background)<sup>7</sup> as well as *VEGF* bitransgenic (*Pax8-rtTA/(tetO)-VEGF*) mice<sup>19</sup> were maintained in a pathogen-free environment. All *in vivo* experiments were performed following approval by the state Animal Protection Board. *Cxcr3*<sup>-/-</sup> and WT littermates were injected with CCl<sub>4</sub> (Merck; 0.6 mL/kg of body weight) intraperitoneally for 6 weeks to induce liver fibrosis. In a separate experiment, recombinant Cxcl9 (1  $\mu$ g; Biomol, Germany) or vehicle was administered to C57BL/6 WT mice concomitantly with or without CCl<sub>4</sub> treatment for 6 weeks. The *in vivo* dose of Cxcl9 was selected based on experience of other chemokines in models of lung fibrosis.<sup>16,18</sup> Mice were sacrificed for analysis 3 days after the last CCl<sub>4</sub> injection. *VEGF* bitransgenic mice were generated by crossbreeding heterozygous *Pax8-rtTA* mice, which express the reverse tetracycline dependent transactivator (rtTA) under control of the Pax promoter, with homozygous (*tetO*)-*VEGF* mice, which synthesize VEGF under the control of a tetracycline responsive promoter. VEGF overexpression in these mice was induced with doxycycline (Dox, 1 mg/mL) orally administered for 14 or 28 days, respectively. Although these mice overexpress VEGF under a kidney-specific promoter, they have strongly increased systemic levels of VEGF (Supporting Fig. 4), which have an impact on other organs of the animals. WT littermates with or without Dox administration were used as controls.

**Quantification of Liver Fibrosis.** Liver scarring was determined by quantitative analysis of Sirius red staining of liver sections (3  $\mu$ m). The area of positive Sirius red staining was quantified using National Institutes of Health (NIH) ImageJ software (<http://rsbweb.nih.gov/>). Hepatic concentrations of the collagen-specific amino acid hydroxyproline were assessed colorimetrically as described.<sup>20</sup>

**Quantification of Angiogenesis.** Angiogenesis was assessed by staining of von Willebrand factor (vWF), CD34, and CD31 (PECAM-1) as well as by SonoVue-enhanced ultrasound. Cryosections of liver tissue were stained with a monoclonal rat antimouse CD31

antibody (BD Biosciences) as well as with a monoclonal goat antihuman vWF antibody (C-20, Santa Cruz) followed by a suitable secondary antibody conjugated with Alexa fluor 488 (Invitrogen) to highlight microvessels. Sections were counterstained for nuclei with Vectashield Mounting Medium with DAPI (Vector Laboratories). Microvessel density (MVD) was determined by counting the CD31 positive vessels in three high-power fields ( $\times 100$  magnification) from areas of highest vascularization.<sup>21</sup> The vWF-positive cells were quantified using NIH ImageJ software. Immunohistochemical staining of the monoclonal rat antimouse CD34 antibody (BD Biosciences) was performed on deparaffinized tissue sections using a routine avidin-biotin-immunoperoxidase technique (Vectastain ABC kit, Vector Laboratories). Before incubation with the primary antibody, tissue sections were subjected to microwave treatment with Citrate-based Antigen Unmasking Solution (Vector Laboratories), followed by a 20-minute cool-down and treatment with 3% hydrogen peroxide. Angiogenesis-related perfusion was assessed by two-dimensional SonoVue-enhanced ultrasound imaging using a clinical imaging system (Acuson S2000, Siemens Healthcare). A multi-D matrix array transducer was attached to a device and the acoustic focus was placed on the level of the dorsal liver capsule. After tail vein injections of mice with 50  $\mu\text{L}$  diluted SonoVue (Bracco; diluted 1:5 with 0.9% NaCl), imaging in CPS-mode with a rate of 13 frames/sec for 40 seconds was performed. A region of interest (ROI) was set within the liver and the area under the curve (AUC) was quantified for this ROI. The values were normalized by the AUC of an ROI placed in the caval vein (Supporting Fig. 1).

**In Vivo Molecular Imaging of VEGFR2.** Fluorescence labeling of VEGFR2 antibody was performed with VivoTag-S680 (VisEn Medical) by way of NHS ester. Normal goat IgG antibody (AF644 and AB-108-C, R&D Systems) was used as isotype control. Antibodies were diluted in 200  $\mu\text{L}$  carbonate/bicarbonate buffer to concentrations of 1 mg/mL and incubated each with 6  $\mu\text{L}$  VivoTag-S680 for 1 hour at room temperature. Nonreacted VivoTag-S680 fluorophores were separated from labeled antibodies by size exclusion chromatography with fast protein liquid chromatography (FPLC) (ÄKTApurifier 10, GE Healthcare). Subsequently, VivoTag-S680 labeled VEGFR2 and IgG probes were injected in  $\text{CCl}_4$ -treated *Cxcr3*<sup>-/-</sup> and WT littermates by way of a tail vein catheter (100  $\mu\text{L}$ ). Probe enrichment in the liver was determined 6 hours after probe injection using fluorescence molecular tomography (FMT 2500; Visen). Additionally, low-

dose  $\mu\text{CT}$  scans (TomoScope DUO, CT Imaging) were performed and coregistered to the 3D FMT data in order to add anatomical information.

**Intrahepatic Protein and Gene Expression.** Isolation of total protein and RNA from snap-frozen liver tissue samples were performed as described.<sup>20</sup> Intrahepatic Cxcl9, Cxcl10, Cxcl1, and VEGF concentrations were determined using mouse enzyme-linked immunosorbent assay (ELISA) kits (R&D Systems), following the manufacturer's instructions. Quantitative reverse-transcription polymerase chain reaction (RT-PCR) was carried out for *VEGF*, *VEGFR1*, *VEGFR2*, and *Colla1* with Assays-on-Demand (Applied Biosystems).

**Analysis of  $\alpha$ -Smooth Muscle Actin ( $\alpha$ -SMA).** Western blotting of  $\alpha$ -SMA on liver protein extracts was performed as described.<sup>20</sup> GAPDH was used as a loading control.

**Intracellular Interferon- $\gamma$  (Ifn- $\gamma$ ) Detection by Flow Cytometry.** Flow cytometric analysis of Ifn- $\gamma$  in the cytoplasm of T cells was performed as described.<sup>7</sup>

**In Vitro Experiments.** Isolation and culture of primary liver cells from  $\text{CCl}_4$ -treated and untreated mice was performed as described by Taura et al.<sup>22</sup> The SV40-transformed mouse endothelial cell line (SVEC) and the stellate cell line GRX<sup>20</sup> were cultured in Dulbecco's modified Eagle's medium (DMEM) with 4.5 g/L glucose (PAA Laboratories) and 10% heat-inactivated fetal calf serum (FCS). For chemokine stimulation, cells were starved in DMEM containing 0.5% FCS (starving medium) for 16 hours and stimulated with recombinant mouse VEGF<sub>164</sub> (20 ng, Biomol) in the presence or absence of recombinant mouse Cxcl9 (100 ng, Biomol) for 10 minutes. Western blots of phosphorylated and total VEGFR2 (KDR, kinase insert domain-containing receptor), PLC $\gamma$  (phospholipase C $\gamma$ ), extracellular signal-regulated kinase (ERK), and c-Jun N-terminal kinase (JNK) (all antibodies from Cell Signaling Technology) were performed.

**Cell Migration Assay.** The chemotaxis of endothelial cells to VEGF and its repression by Cxcl9 was assessed in a modified Boyden chamber system. Endothelial cells ( $1 \times 10^4$ ) were placed in the upper compartment in starving medium and were exposed to recombinant mouse VEGF<sub>164</sub> (20 ng, Biomol) alone or in combination with recombinant mouse Cxcl9 (100 ng) in the lower compartment. After 4 hours of incubation, cell migration was analyzed by counting cells of three random high-power fields ( $\times 100$  magnification). All experiments were performed in quadruplicate.

**Cell Proliferation Assay.** For quantification of endothelial and stellate cell proliferation a

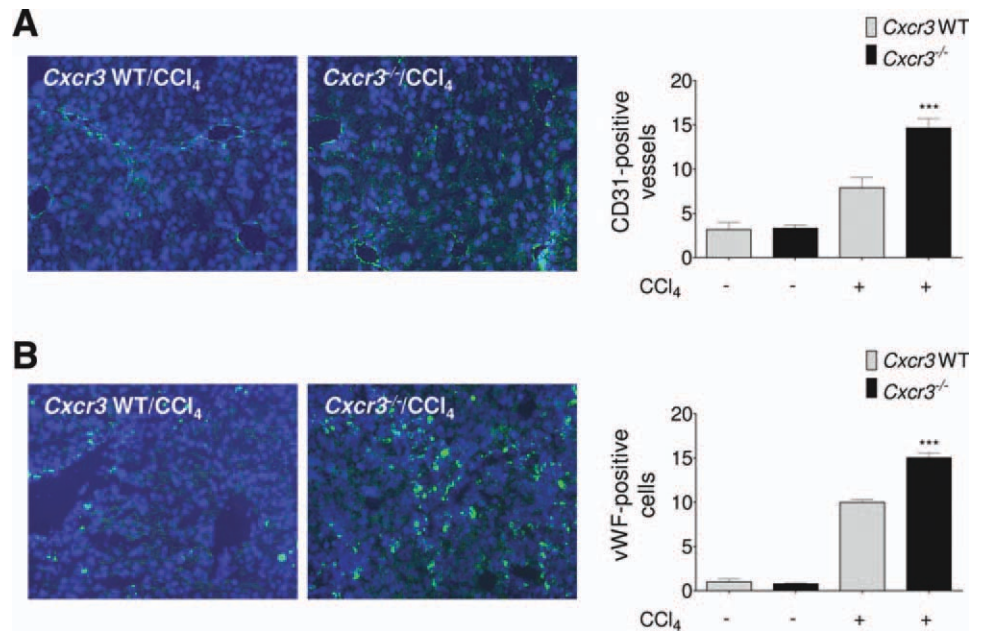


Fig. 1. Association of neoangiogenesis with experimental liver fibrosis. Vessel density was assessed by counting CD31-positive vessels ( $\times 200$  magnification) after immunofluorescence staining of CD31 (A) and vWF (B). The administration of CCl<sub>4</sub> for 6 weeks led to a significantly increased number of CD31 and vWF-positive vessels in Cxcr3<sup>-/-</sup> mice compared with their WT littermates (n = 8 mice per group).

chemiluminescent immunoassay based on the measurement of bromodeoxyuridine (BrdU) incorporation during DNA synthesis was used (Cell Proliferation ELISA, BRDU, Roche Applied Science).<sup>20</sup> Briefly, cells ( $0.5 \times 10^4$ ) were cultured in starving medium for 16 hours and stimulated for 24 hours with VEGF and costimulated with Cxcl9 as mentioned. After BrdU labeling, fixation, and DNA denaturation, the BrdU incorporation was quantified by measuring the subsequent substrate reaction. For studying sinusoidal endothelial cell / hepatic stellate cell interactions in response to Cxcl9, we performed experiments with conditioned medium. Cultured endothelial cells were stimulated with or without VEGF  $\pm$  Cxcl9 (see above) for 24 hours and the supernatant was harvested for cell migration and proliferation experiments of stellate cells.

**Assessment of Cell Proliferation and Migration in a Scratch Assay.** The composite of endothelial cell migration and proliferation were performed in a scratch assay. After the cell culture was confluent in 6-well plates, a straight scratch with a pipette tip (blue, Gilson) was created on the cell monolayer. Subsequently, the cells were stimulated for 24 hours with VEGF in the presence or absence of recombinant Cxcl9. To quantify cell migration and proliferation the width of the scratch was recorded and measured digitally ( $\times 100$  magnification) before and after stimulation in order to calculate the ratio.

**In Vitro Matrigel Angiogenesis Assay.** To study angiogenesis, the process of blood vessels, *in vitro*, a Matrigel Basement Membrane Matrix (BD Biosciences) was used. Endothelial cells ( $5 \times 10^4$ ) were plated

on Matrigel in starving medium and stimulated for 8 hours with VEGF and costimulated with Cxcl9 as mentioned. The tube formation under these conditions was quantified by measuring the number of these capillary-like structures.

**Statistical Analysis.** Results are depicted as mean  $\pm$  standard error of the mean (SEM). Statistical significance was assessed by two-way analysis of variance followed by Student *t* test, with Welch's correction in case of unequal variances. Statistical analyses were performed using GraphPad Prism 5.

## Results

**Lack of Cxcr3 Is Associated with Increased Neoangiogenesis in Experimental Liver Fibrosis.** We first assessed the density of intrahepatic blood vessels in WT mice with or without administration of CCl<sub>4</sub> for 6 weeks.

Development of liver fibrosis after CCl<sub>4</sub> challenge was associated with an increased number of CD31 and vWF-positive vessels and augmented hepatic messenger RNA (mRNA) expression of VEGF and VEGFR2, confirming a link between angiogenesis and progression of liver fibrosis.<sup>22</sup> Treatment with CCl<sub>4</sub> also increased hepatic protein concentrations of angiogenic (Cxcl1) and angiostatic (Cxcl9, Cxcl10) chemokines (Supporting Fig. 2). Notably, Cxcr3<sup>-/-</sup> mice displayed a further significantly higher blood vessel density within the liver compared with their WT littermates after CCl<sub>4</sub> treatment (Fig. 1A,B). Aberrant angiogenesis in Cxcr3<sup>-/-</sup> mice was also reflected by strongly

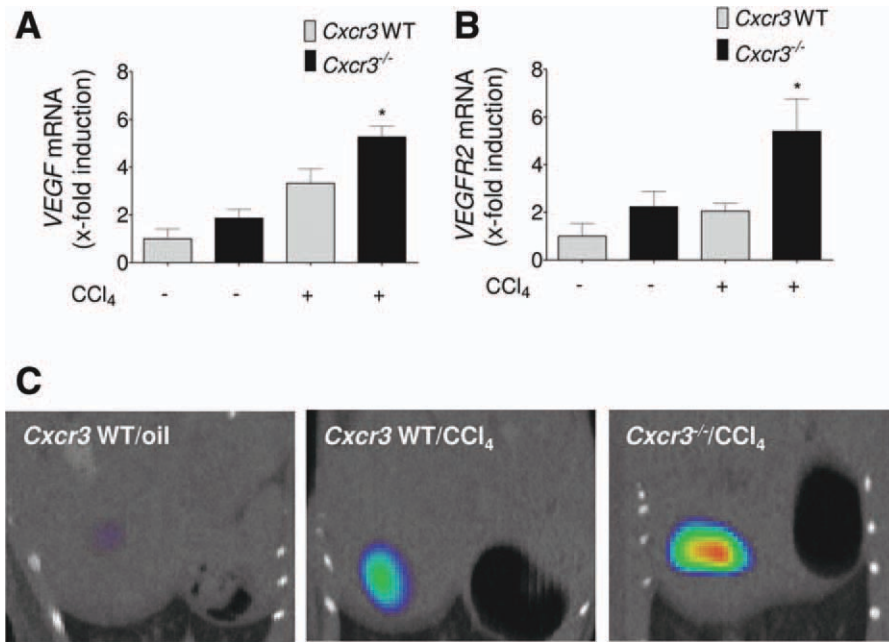


Fig. 2. Increased neoangiogenesis in  $Cxcr3^{-/-}$  mice is associated with a significantly increased mRNA expression of VEGF (A) and VEGFR2 (B) compared with their WT littermates. The augmented expression of VEGFR2 in  $Cxcr3^{-/-}$  mice was confirmed *in vivo* by fluorescence molecular tomography using radiolabeled antibodies against VEGFR2 (C) (see Materials and Methods for details). \* $P < 0.05$ .

increased levels of *VEGF* and *VEGFR2* mRNA expression (Fig. 2A,B). Interestingly, the increased expression of *VEGF* receptors in  $Cxcr3^{-/-}$  mice was only evident for *VEGFR2*, but not for *VEGFR1* (data not shown). Given the importance of the VEGF pathway in angiogenesis,<sup>14</sup> we established a fluorescence molecular tomography (FMT) detection method for assessment of VEGFR2 expression *in vivo*. The FMT confirmed a higher level of VEGFR2 in the livers of  $Cxcr3^{-/-}$  mice compared with untreated mice and WT littermates after 6 weeks of CCl<sub>4</sub> treatment (Fig. 2C). Enhanced overall neoangiogenesis in  $Cxcr3^{-/-}$  mice was further confirmed by increased perfusion of the liver by contrast-enhanced ultrasound (Supporting Fig. 3), supporting a high vessel density and a strong proangiogenic phenotype of  $Cxcr3^{-/-}$  mice.

**VEGF Overexpression Is Associated with Augmented Fibrogenesis and Increased Concentrations of Chemokines.** In light of the increased VEGF/VEGFR2 expression in CCl<sub>4</sub>-treated mice, we next evaluated the direct effects of VEGF on the liver. *VEGF* bitransgenic mice received doxycycline for 2 and 4 weeks, resulting in strongly increased serum concentrations of VEGF in these animals (Supporting Fig. 4A). Under these experimental conditions, overexpression of VEGF for 4 weeks was associated with increased new vessel formation within the liver (Supporting Fig. 4B) and increased hepatic collagen deposition (Sirius red staining, Fig. 3A). In line with these changes, overexpression of VEGF also resulted in a time-dependent increase of hydroxyproline, a collagen-specific amino acid, and *Col1a1* mRNA within the liver (Fig. 3B,C).

As depicted in Fig. 2E,F, overexpression of VEGF was also associated with altered hepatic levels of Cxc chemokines. As in CCl<sub>4</sub>-treated mice (Supporting Fig. 2), the angiogenic chemokine Cxcl1 (Supporting Fig. 4C) and the angiostatic chemokine Cxcl9 (Fig. 3D) were highly abundant within the liver in response to VEGF overexpression.

**Angiostatic Chemokine Cxcl9 Directly Abrogates VEGF Effects In Vitro.** Because the *in vivo* results suggested a close association between VEGF pathways and the expression of chemokines, we next assessed the direct effects of the angiostatic chemokine Cxcl9 on VEGF-mediated effects on endothelial cells and stellate cells *in vitro*. Both cell types are considered to be involved in neoangiogenesis within the liver<sup>14</sup> and express both Cxcl9 and its receptor *Cxcr3* (Supporting Fig. 5A,B). As depicted in Fig. 4A,B, Cxcl9 significantly abrogated the proliferative and migratory response of VEGF on endothelial cells. We next assessed direct functional aspects of Cxcl9 on angiogenesis in a Matrigel assay. As shown in Fig. 4C, Cxcl9 indeed strongly abrogated endothelial network formation, supporting its direct involvement in VEGF-induced vessel formation. Furthermore, Cxcl9 inhibited the scratch closure in a functional scratch assay, which is also considered as a combination of proliferation and migration of endothelial cells (Supporting Fig. 5C). Importantly, the inhibitory effects of Cxcl9 were also found in primary sinusoidal endothelial cells isolated from livers of CCl<sub>4</sub> damaged animals (Fig. 5A,B), supporting the relevance of our findings for the injury model used in our study. On a

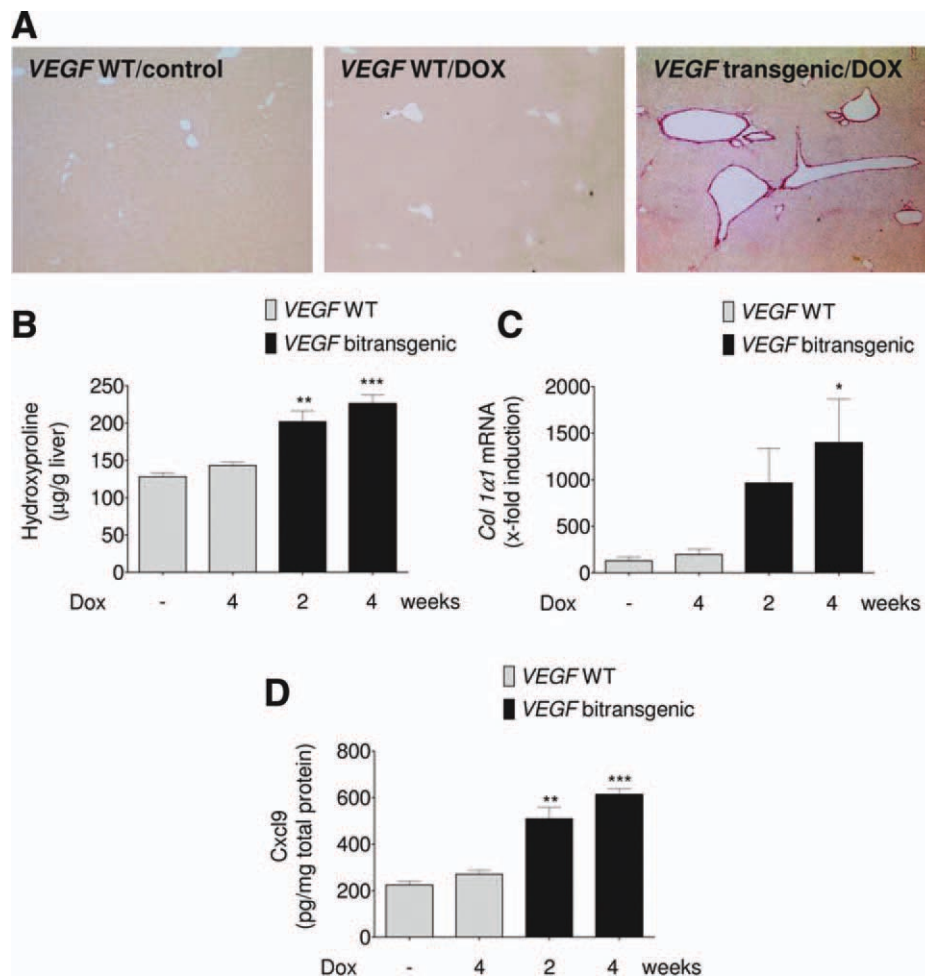


Fig. 3. The systemic overexpression of VEGF for 4 weeks leads to an augmented deposition of collagen (Sirius red staining, magnification  $\times 100$ ) (A). The increased fibrogenic response in VEGF overexpression animals was confirmed by a time-dependent increase of the collagen-specific amino acid hydroxyproline (B) and the mRNA expression of *Col1a1* (C). Furthermore, VEGF overexpression is associated with increased levels of the chemokine Cxcl9 (D) within the liver ( $n = 8$  mice per group). \* $P < 0.05$ , \*\* $P < 0.01$ , \*\*\* $P < 0.001$ .

molecular level, the effects of Cxcl9 were associated with a reduced phosphorylation of VEGFR2 (KDR), its downstream mediator PLC $\gamma$ , JNK, and ERK in primary endothelial cells (Fig. 5C), supporting earlier results of antiangiogenic chemokines on the VEGF signaling pathway.<sup>17</sup> Cxcl9 also reduced the VEGF-induced proliferation of stellate cells (Supporting Fig. 6A), which was also associated with a reduced phosphorylation of KDR, JNK, and ERK (Supporting Fig. 6B). As endothelial and stellate cells are both considered to play a pivotal role during liver neoangiogenesis, we also evaluated the direct interaction between these cell types with and without treatment of Cxcl9. Indeed, conditioned medium from VEGF stimulated endothelial cells induced the proliferation and migration of stellate cells *in vitro*, which was strongly reduced by concomitant treatment of endothelial cells with Cxcl9 (Supporting Fig. 6C).

**Cxcl9 Inhibits Neoangiogenesis in the Liver In Vivo.** In the light of these *in vitro* data, we hypothesized that systemic administration of Cxcl9 might also modulate CCl<sub>4</sub>-induced hepatic neoangiogenesis

*in vivo*. Indeed, daily administration of Cxcl9 concomitantly to CCl<sub>4</sub> strongly inhibited the formation of new blood vessels compared with vehicle-treated mice. The difference between Cxcl9 and vehicle-treated mice was evident by quantification of CD31-positive cells (Fig. 6A) as well as vWF-positive cells (Supporting Fig. 7). Furthermore, as determined by contrast-enhanced ultrasound, the microvascular perfusion of the liver was significantly reduced in Cxcl9-treated mice compared with vehicle-treated mice, supporting a reduced density of vessels in the livers of these mice (Fig. 6B). In line with the direct interaction between Cxcl9 and VEGF pathways *in vitro*, the antiangiogenic properties of Cxcl9 were also linked to a strong decrease in VEGF protein levels within the liver *in vivo* (Supporting Fig. 8A).

**Treatment of Mice with Cxcl9 Ameliorates Liver Fibrosis In Vivo.** Importantly, alongside reduced neoangiogenesis, mice treated with Cxcl9 also had a strongly reduced severity of liver fibrosis compared with vehicle-treated mice (Fig. 7A). This difference was evident after quantification of Sirius red-stained

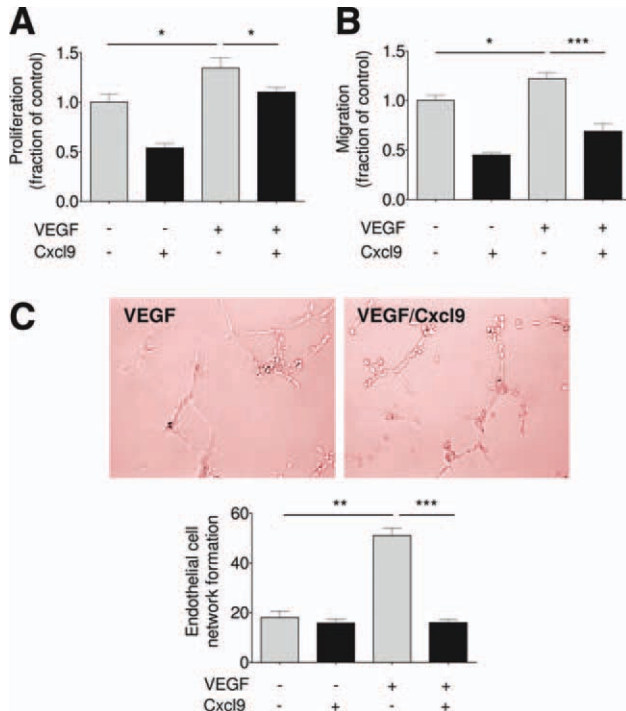


Fig. 4. *In vitro*, Cxcl9 counteracts VEGF-mediated endothelial cell (SVEC) proliferation (A) and migration (B). Furthermore, Cxcl9 inhibits the endothelial cell network formation in a Matrigel assay (C). \* $P < 0.05$ , \*\* $P < 0.01$ , \*\*\* $P < 0.001$ .

liver tissues (Fig. 7B), biochemical measurement of hepatic hydroxyproline contents (Fig. 7C), and by assessment of intrahepatic *Collα1* mRNA expression (Supporting Fig. 8B). As Cxcl9 might have direct chemotactic effects on liver infiltrating cells, we also determined the number of  $T_H1$ -polarized, IFN- $\gamma$ -positive cells in the livers of Cxcl9 and vehicle-treated

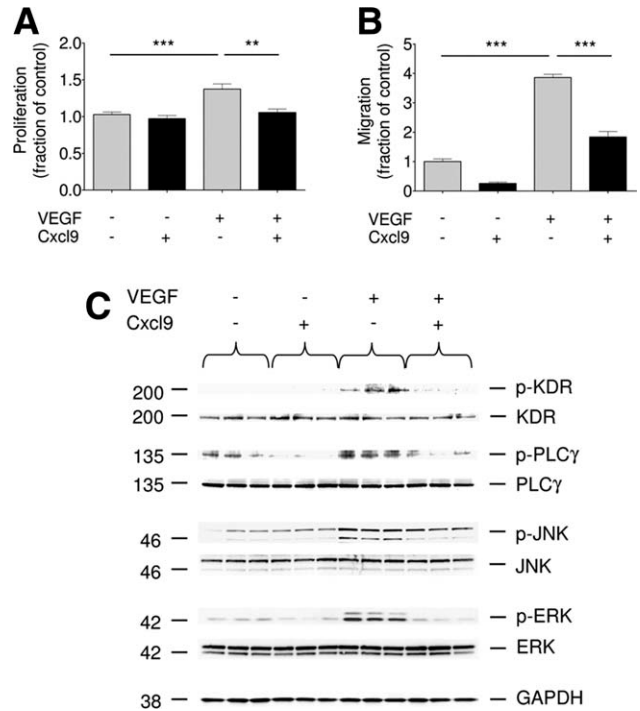


Fig. 5. Cxcl9 does inhibit primary liver sinusoidal endothelial cell proliferation (A) and migration (B) after isolation of the cells from livers challenged with  $CCl_4$  *in vivo*. The *in vitro* effects of Cxcl9 are mediated by strong repression of phosphorylation of VEGFR2 (KDR) and its downstream modulator PLC $\gamma$ , suggesting a direct effect of the chemokine on the VEGF signaling cascade. Furthermore, Cxcl9 inhibits phosphorylation of JNK and ERK (C). \*\* $P < 0.01$ , \*\*\* $P < 0.001$ .

mice. However, the number of IFN- $\gamma$ -positive cells was not different between the groups (Supporting Fig. 8C), arguing against a major influence of the immune system on the phenotype observed after Cxcl9 treatment. Instead, the content of  $\alpha$ -SMA in the liver was

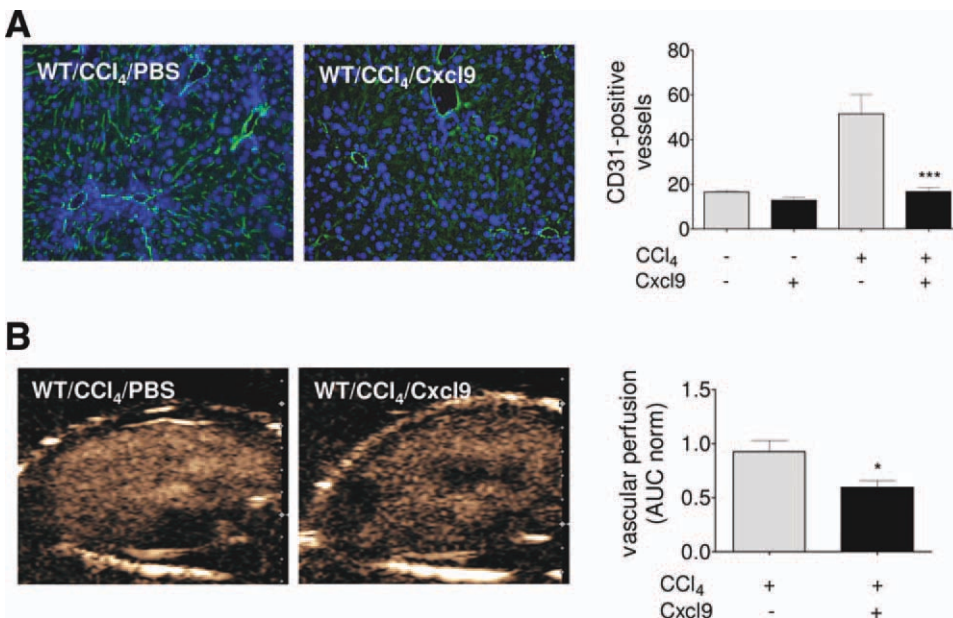


Fig. 6. *In vivo* inhibition of angiogenesis by systemic Cxcl9. The angiostatic potential of Cxcl9 was validated in the experimental liver fibrosis model by CD31 staining (magnification  $\times 200$ ) (A). These results are supported by reduced perfusion of the liver as determined by contrast-enhanced ultrasound imaging (B) (see Materials and Methods for details). \* $P < 0.05$ , \*\*\* $P < 0.001$ .

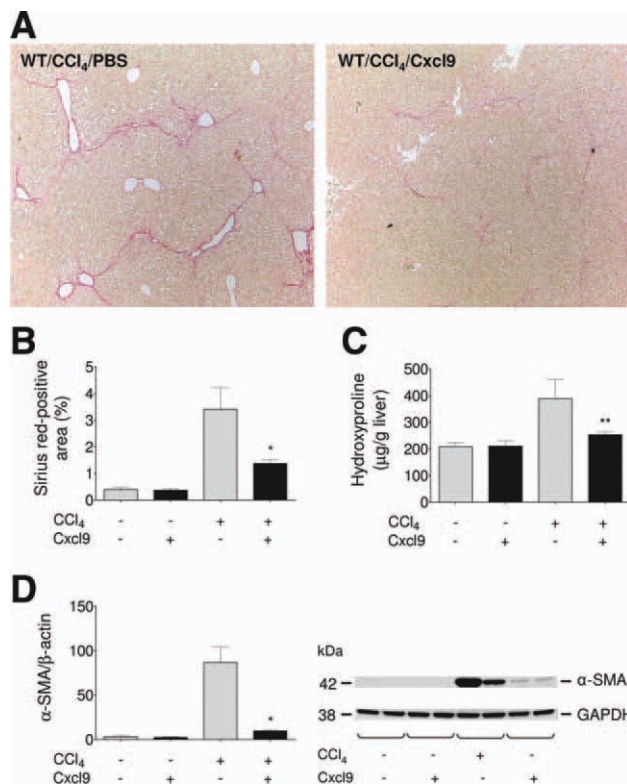


Fig. 7. Cxcl9 therapy ameliorates liver fibrosis *in vivo*. Representative Sirius red stainings of CCl<sub>4</sub>-treated WT mice, with a concomitant administration of vehicle or Cxcl9 ( $n = 9$  per group;  $\times 100$  magnification) (A). Reduced fibrosis in Cxcl9-treated mice was evident by a significantly lower Sirius red-positive area (B) and decreased concentrations of hydroxyproline (C). Western blot analysis demonstrates a reduced  $\alpha$ -Sma protein expression in total liver lysates of Cxcl9-treated mice compared with vehicle-treated mice (D). \* $P < 0.05$ , \*\* $P < 0.01$ .

strongly reduced by Cxcl9 treatment (Fig. 7D), suggesting that a main effect of Cxcl9 *in vivo* is the modulation of stellate cell activation alongside with reduced neoangiogenesis and endothelial cell inhibition.

## Discussion

In the current study we provide evidence that the Cxcr3 chemokine system is an important modulator of neoangiogenesis in the murine liver and that the Cxcr3 ligand Cxcl9 has the potential to ameliorate neoangiogenesis and liver fibrosis *in vivo*.

In recent studies we demonstrated that mice deficient in the chemokine receptor *Cxcr3* are more prone to liver fibrosis in different experimental models.<sup>7</sup> These results were in line with earlier findings of the importance of Cxcr3 in models of pulmonary and renal fibrosis.<sup>12,13</sup> The effects of Cxcr3 ligands in liver disease models were mainly explained by reduced recruitment of T<sub>H</sub>1-polarized or regulatory T cells.<sup>7,10,11</sup> Furthermore, a direct inhibitory effect of

CXCL9 on collagen secretion of stellate cells was identified.<sup>7</sup> However, another important feature of Cxcr3 ligands is their strong angiostatic function<sup>16,23</sup> and their close correlations to VEGF concentrations *in vivo*.<sup>24</sup> These results, together with the emerging knowledge of the importance of angiogenesis in chronic liver diseases,<sup>14</sup> motivated our interest to assess the functional role of the Cxcr3 chemokine system in angiogenesis during experimental liver damage.

In the first set of experiments we confirmed that an increased number of vessels within the liver is a characteristic feature of experimental liver fibrosis. In the CCl<sub>4</sub> model, vessel formation was associated with strong expression of the pivotal proangiogenic growth factor VEGF and its receptor VEGFR2, which have been earlier considered a prerequisite for fibrogenesis *in vivo*.<sup>25</sup> Notably, all of these features were strongly augmented in *Cxcr3*<sup>-/-</sup> mice compared with their WT littermates, providing the first evidence that this chemokine pathway displays a nonredundant functional role in liver neoangiogenesis. As angiogenic as well as angiostatic chemokines were induced by CCl<sub>4</sub>, we speculate that the increased expression of the Cxcr3 ligands Cxcl9 and Cxcl10 are part of a feedback loop in response to liver damage. However, as angiogenesis and fibrosis are considered to develop in parallel in chronically damaged liver,<sup>26</sup> the question of a primary effect of Cxcr3 ligands on angiogenesis or fibrogenesis remains obscure at this point. We therefore used a bitransgenic mouse model with a strong systemic overexpression of VEGF to further assess the direct impact of this angiogenic growth factor on liver fibrogenesis and intrahepatic chemokine expression. VEGF overexpression indeed led to a fibrogenic tissue response within the liver as determined by significantly increased Col1a1 mRNA and hydroxyproline concentrations, although frank scar formation was not evident after 4 weeks by Sirius red staining. Notably, VEGF overexpression also strongly increased intrahepatic concentrations of Cxcl9, suggesting a functional feedback loop between the molecules. As CXCR3 agonists in humans have been shown to directly interfere with VEGF signaling,<sup>17,27</sup> we next assessed whether there is a direct biological interaction between VEGF and Cxcl9 on target cells. Indeed, Cxcl9 repressed proliferative and migratory effects as well as tube formation of VEGF-stimulated endothelial cells. As Cxcl9 does not directly inhibit VEGF secretion from liver cells (data not shown), these effects appear to be mediated by direct interference of Cxcl9 with the VEGF signaling pathway, as described for Cxcl4.<sup>27</sup> As endothelial and stellate cells are considered strong contributors to

angiogenesis and fibrogenesis,<sup>22,28</sup> we also evaluated the inhibitory potential of Cxcl9 on the interaction between these cell types. Indeed, Cxcl9-treated endothelial cells were less potent in inducing stellate cell migration and proliferation. Because these *in vitro* results suggested a possible direct effect of Cxcl9 on multiple aspects of chronic liver damage, we next assessed the feasibility of amelioration of liver damage *in vivo* by therapeutic application of Cxcl9. Although such a translational approach has been performed in lung injury models,<sup>18</sup> the use of a chemokine for modulating chronic liver injury has not yet been systematically evaluated. In these crucial experiments, therapy with Cxcl9 indeed led to a reduction of CD31-positive vessels within the liver. The antiangiogenic changes in the Cxcl9 treated animals were confirmed by a reduced vascular liver perfusion as determined by contrast-enhanced ultrasound. As Cxcl9 is not likely to have substantial effects on cardiac output, the reduced perfusion can be considered a marker of reduced vessel density within the liver. In future studies the ultrasound examination established in our study might therefore be used for the longitudinal evaluation of vessel density during experimental angiostatic therapies.<sup>29</sup> It is important to note that inhibition of angiogenesis by targeting key proangiogenic molecules has been shown to aggravate liver fibrosis under certain circumstances.<sup>30,31</sup> We therefore systematically assessed the fibrotic phenotype in the Cxcl9-treated mice compared with vehicle-treated mice. As shown in Fig. 6, amelioration of angiogenesis in our model was associated with strongly reduced scar formation in the liver. As we could not find major differences in inflammation between Cxcl9 and vehicle-treated mice, which might as such influence angiogenesis,<sup>32</sup> the amelioration of liver fibrosis seems to be primarily due to reduced stellate and endothelial cell activation with a corresponding reduction in vessel formation. Indeed, other drugs that mainly target stellate and endothelial cells have also been shown to improve liver fibrosis *in vivo*.<sup>28,33</sup>

Taken together, our findings present evidence that the Cxcr3 ligand Cxcl9 is a strong counter-regulatory molecule of VEGF-driven aberrant liver vascularization and perfusion *in vitro* and *in vivo*. The results describe novel features of this ELR-negative chemokine within the liver and set the stage for further evaluation of Cxcl9 as a potential therapeutic option in liver diseases associated with enhanced angiogenesis and fibrosis.

## References

- Friedman SL. Mechanisms of hepatic fibrogenesis. *Gastroenterology* 2008;134:1655-1669.
- Corpechot C, Barbu V, Wendum D, Kinnman N, Rey C, Poupon R, et al. Hypoxia-induced VEGF and collagen I expressions are associated with angiogenesis and fibrogenesis in experimental cirrhosis. *HEPATOLOGY* 2002;35:1010-1021.
- Medina J, Arroyo AG, Sanchez-Madrid F, Moreno-Otero R. Angiogenesis in chronic inflammatory liver disease. *HEPATOLOGY* 2004;39:1185-1195.
- Garcia-Tsao G, Friedman S, Iredale J, Pinzani M. Now there are many (stages) where before there was one: in search of a pathophysiological classification of cirrhosis. *HEPATOLOGY* 2010;51:1445-1449.
- Keeley EC, Mehrad B, Strieter RM. Chemokines as mediators of neovascularization. *Arterioscler Thromb Vasc Biol* 2008;28:1928-1936.
- Sahin H, Trautwein C, Wasmuth HE. Functional role of chemokines in liver disease models. *Nat Rev Gastroenterol Hepatol* 2010;7:682-690.
- Wasmuth HE, Lammert F, Zaldivar MM, Weiskirchen R, Hellerbrand C, Scholten D, et al. Antifibrotic effects of CXCL9 and its receptor CXCR3 in livers of mice and humans. *Gastroenterology* 2009;137:309-319, 319 e301-303.
- Wynn TA. Fibrotic disease and the T(H)1/T(H)2 paradigm. *Nat Rev Immunol* 2004;4:583-594.
- Schrage A, Wechsung K, Neumann K, Schumann M, Schulzke JD, Engelhardt B, et al. Enhanced T cell transmigration across the murine liver sinusoidal endothelium is mediated by transcytosis and surface presentation of chemokines. *HEPATOLOGY* 2008;48:1262-1272.
- Santodomingo-Garzon T, Han J, Le T, Yang Y, Swain MG. Natural killer T cells regulate the homing of chemokine CXC receptor 3-positive regulatory T cells to the liver in mice. *HEPATOLOGY* 2009;49:1267-1276.
- Erhardt A, Wegscheid C, Claass B, Carambia A, Herkel J, Mittrucker HW, et al. CXCR3 deficiency exacerbates liver disease and abrogates tolerance in a mouse model of immune-mediated hepatitis. *J Immunol* 2011;186:5284-5293.
- Jiang D, Liang J, Hodge J, Lu B, Zhu Z, Yu S, et al. Regulation of pulmonary fibrosis by chemokine receptor CXCR3. *J Clin Invest* 2004;114:291-299.
- Nakaya I, Wada T, Furuichi K, Sakai N, Kitagawa K, Yokoyama H, et al. Blockade of IP-10/CXCR3 promotes progressive renal fibrosis. *Nephron Exp Nephrol* 2007;107:e12-21.
- Thabut D, Shah V. Intrahepatic angiogenesis and sinusoidal remodeling in chronic liver disease: new targets for the treatment of portal hypertension? *J Hepatol* 2010;53:976-980.
- Fernandez M, Semela D, Bruix J, Colle I, Pinzani M, Bosch J. Angiogenesis in liver disease. *J Hepatol* 2009;50:604-620.
- Strieter RM, Burdick MD, Gomperts BN, Belperio JA, Keane MP. CXC chemokines in angiogenesis. *Cytokine Growth Factor Rev* 2005;16:593-609.
- Sulpice E, Bryckaert M, Lacour J, Contreres JO, Tobelem G. Platelet factor 4 inhibits FGF2-induced endothelial cell proliferation via the extracellular signal-regulated kinase pathway but not by the phosphatidylinositol 3-kinase pathway. *Blood* 2002;100:3087-3094.
- Keane MP, Belperio JA, Arenberg DA, Burdick MD, Xu ZJ, Xue YY, et al. IFN-gamma-inducible protein-10 attenuates bleomycin-induced pulmonary fibrosis via inhibition of angiogenesis. *J Immunol* 1999;163:5686-5692.
- Hakrout S, Moeller MJ, Theilig F, Kaissling B, Sijmonsma TP, Jugold M, et al. Effects of increased renal tubular vascular endothelial growth factor (VEGF) on fibrosis, cyst formation, and glomerular disease. *Am J Pathol* 2009;175:1883-1895.
- Berres ML, Koenen RR, Rueland A, Zaldivar MM, Heinrichs D, Sahin H, et al. Antagonism of the chemokine Ccl5 ameliorates experimental liver fibrosis in mice. *J Clin Invest* 2010;120:4129-4140.
- Weidner N. Intratumor microvessel density as a prognostic factor in cancer. *Am J Pathol* 1995;147:9-19.
- Taura K, De Minicis S, Seki E, Hatano E, Iwaisako K, Osterreicher CH, et al. Hepatic stellate cells secrete angiopoietin 1 that induces angiogenesis in liver fibrosis. *Gastroenterology* 2008;135:1729-1738.
- Campanella GS, Colvin RA, Luster AD. CXCL10 can inhibit endothelial cell proliferation independently of CXCR3. *PLoS One* 2010;13:5:e12700.

24. Wakabayashi Y, Usui Y, Okunuki Y, Kezuka T, Takeuchi M, Goto H, et al. Correlation of vascular endothelial growth factor with chemokines in the vitreous in diabetic retinopathy. *Retina* 2010;30:339-344.
25. Yoshiji H, Kuriyama S, Yoshii J, Ikenaka Y, Noguchi R, Hicklin DJ, et al. Vascular endothelial growth factor and receptor interaction is a prerequisite for murine hepatic fibrogenesis. *Gut* 2003;52:1347-1354.
26. Lee JS, Semela D, Iredale J, Shah VH. Sinusoidal remodeling and angiogenesis: a new function for the liver-specific pericyte? *HEPATOLOGY* 2007;45:817-825.
27. Sulpice E, Contreres JO, Lacour J, Bryckaert M, Tobelem G. Platelet factor 4 disrupts the intracellular signalling cascade induced by vascular endothelial growth factor by both KDR dependent and independent mechanisms. *Eur J Biochem* 2004;271:3310-3318.
28. Tugues S, Fernandez-Varo G, Munoz-Luque J, Ros J, Arroyo V, Rodes J, et al. Antiangiogenic treatment with sunitinib ameliorates inflammatory infiltrate, fibrosis, and portal pressure in cirrhotic rats. *HEPATOLOGY* 2007;46:1919-1926.
29. Shah VH, Bruix J. Antiangiogenic therapy: not just for cancer anymore? *HEPATOLOGY* 2009;49:1066-1068.
30. Patsenker E, Popov Y, Stickel F, Schneider V, Ledermann M, Sagesser H, et al. Pharmacological inhibition of integrin alphavbeta3 aggravates experimental liver fibrosis and suppresses hepatic angiogenesis. *HEPATOLOGY* 2009;50:1501-1511.
31. Stockmann C, Kerdiles Y, Nomaksteinsky M, Weidemann A, Takeda N, Doedens A, et al. Loss of myeloid cell-derived vascular endothelial growth factor accelerates fibrosis. *Proc Natl Acad Sci U S A* 2010;107:4329-4334.
32. Jackson JR, Seed MP, Kircher CH, Willoughby DA, Winkler JD. The codependence of angiogenesis and chronic inflammation. *FASEB J* 1997;11:457-465.
33. Mejias M, Garcia-Pras E, Tiani C, Miquel R, Bosch J, Fernandez M. Beneficial effects of sorafenib on splanchnic, intrahepatic, and portocolateral circulations in portal hypertensive and cirrhotic rats. *HEPATOLOGY* 2009;49:1245-1256.